Liquid Crystals
Publication details, including instructions for authors and subscription information:
http://www.informaworld.com/smpp/title~content=t713926090

Synthesis and characterization of new chiral liquid crystalline polyacrylates from L-isoleucine

Olga M. S. Ritter; Aloir A. Merlo; Fabiano V. Pereira; Nadya P. Da Silveira; Erik Geissler; J. Zukerman-Schpector

To cite this Article Ritter, Olga M. S. , Merlo, Aloir A. , Pereira, Fabiano V. , Da Silveira, Nadya P. , Geissler, Erik and Zukerman-Schpector, J.(2002) 'Synthesis and characterization of new chiral liquid crystalline polyacrylates from L-isoleucine', Liquid Crystals, 29: 9, 1187 — 1200

To link to this Article: DOI: 10.1080/02678290210156678

URL: http://dx.doi.org/10.1080/02678290210156678

LIQUID CRYSTALS, 2002, VOL. 29, NO. 9, 1187–1200

Taylor & Francis
Taylor & Francis Group

Synthesis and characterization of new chiral liquid crystalline polyacrylates from L-isoleucine

OLGA M. S. RITTER†, ALOIR A. MERLO†*, FABIANO V. PEREIRA†,
NADYA P. DA SILVEIRA†‡, ERIK GEISSLER‡ and
J. ZUKERMAN-SCHPECTOR§

†Instituto de Química, Universidade Federal do Rio Grande do Sul,
Av. Bento Gonçalves 9500, CEP 91501-970, Porto Alegre, Brazil
‡Laboratoire de Spectrométrie Physique, Université Joseph Fourier de Grenoble,
France
§Laboratório de Cristalografia, Estereodinâmica e Modelagem Molecular,
Departamento de Química,
Universidade Federal de São Carlos and Instituto de Química, USP, Brazil

(*Received 1 September 2001; in final form 1 April 2002; accepted 9 April 2002*)

The synthesis of chiral side chain liquid crystalline polyacrylates with a two-stereogenic centre from L-α-aminoacid is described. The chiral tail is 2-chloroalcohol obtained from L-isoleucine and the spacer group has either four or eleven methylene units. The mesogenic moiety is derived from phenyl benzoate. The stereochemistry of the key intermediate (2*S*,3*S*)-(+)-4-[1-(2-chloro-3-methyl)pentyloxy]phenyl benzoate (**6**) obtained by a Mitsunobu reaction was established by single crystal X-ray analysis. This result indicates that the nucleophilic displacement of chiral diazonium salts proceeds with overall retention of configuration. The liquid crystalline behaviour of polyacrylates **P13** and **P14** was investigated by DSC, optical microscopy, small angle X-ray scattering and depolarized light scattering. The polyacrylate **P13**, with eleven methylene units in the spacer, exhibits a chiral smectic A phase whereas the polyacrylate **P14**, with a spacer containing four methylene units, displays a chiral nematic phase.

1. Introduction

Since 1978, when Ringsdorf and co-workers [1] developed a new architecture for polymers entitled *side chain liquid crystal polymer* (SCLCP), research in basic liquid crystalline science and technological applications has experienced great growth. This intense interest is due to their wide range of applications as 'hightech' materials [2, 3]. Moreover, chirality in smectic liquid crystals (LCs) gained a pivotal position in the history of LCs after Meyer and co-workers [4] discovered the phenomenon of ferroelectricity in chiral SmC LCs and, later, Clark and Largerwall [5] found a new electro-optical effect with surface stabilized ferroelectric liquid crystals (SSFLCs). However, the first chiral side chain liquid crystal polymer was reported in 1984 by Shibaev and co-workers [6]. Since then, a wide range of candidate materials has been synthesized and their mesomorphic and electro-optical properties studied [7].

In a previous paper, we reported the synthesis and mesomorphic behaviour of a series of achiral liquid crystalline polyacrylates possessing a short spacer with four methylene units [8]. More recently, we described the synthesis of new chiral polyacrylates derived from (*S*)-2-methyl-1-butanol as chiral terminal chain, with spacer groups having either four or eleven carbon atoms [9]. Their mesomorphic behaviour was investigated and their properties in solution were studied by light scattering. The phase behaviour was dependent on the molecular relationships among the polymer backbone, the terminal group attached to mesogenic groups and the molecular mass. The polyacrylate with four methylene units in the spacer exhibits a chiral nematic phase, whereas the polyacrylate with a spacer containing eleven methylene units displays a smectic phase.

In this paper we report the synthesis of chiral side chain liquid crystal polyacrylates **P13** and **P14** containing (2*S*,3*S*)-4′-[1-(2-chloro-3-methyl)pentyloxy]phenyl 4-[1-(propenoyloxy)alkyloxy]benzoates (**M9** and **M12**) and their mesomorphic properties. The new chiral terminal chain is derived from L-isoleucine, and the relative and absolute stereochemical relationships were established unequivocally by single crystal X-ray analysis. The chemical structure of the new polyacrylates is shown in figure 1. Their liquid crystalline properties were

---

*Author for correspondence; e-mail: aloir@iq.ufrgs.br

Liquid Crystals ISSN 0267-8292 print/ISSN 1366-5855 online © 2002 Taylor & Francis Ltd
http://www.tandf.co.uk/journals
DOI: 10.1080/02678290210156678

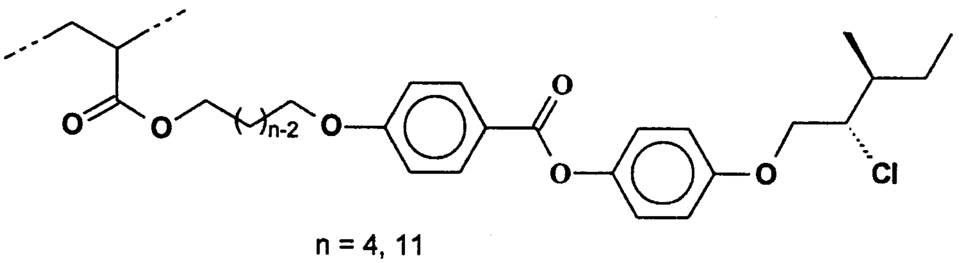

Figure 1. General chemical structure of the chiral liquid crystal polyacrylates.

systematically studied by detailed small angle X-ray scattering as well as by differential scanning calorimetry and polarizing optical microscopy. The mesophase behaviour and molecular orientation in the mesophase of **P13** were also investigated by depolarized light scattering.

A variety of chiral groups is already used in chiral liquid crystalline compounds [10]. We believe that the chiral precursors **3** and **7** that were synthesized in this work are promising candidates for generating both low and high molar mass chiral LCs. The features of **3** or **7** as a chiral group in liquid crystalline compounds are: (i) they are easily prepared with excellent stereochemical integrity from readily available amino acids; (ii) the chiral centre near an aromatic core or carboxylate group, as well as the highly polar C–Cl bond and *gauche* effect [11] around the C_1 and C_2 carbon bond, lead us to expect enhancement of the electro-optical properties.

2. Experimental

^{1}H NMR and ^{13}C NMR spectra in $CDCl_3$ were obtained using Varian-200 and 300 MHz spectrometers using TMS as the internal standard. IR spectra were recorded in Nujol on a 3000 Galaxy Series spectrometer. Elemental analysis was determined using a Perkin Elmer 2400CHN instrument. Optical rotations were recorded on a Perkin-Elmer 341 polarimeter at the sodium D line. The thermal transitions and the mesomorphic textures were determined using a Leitz Ortholux polarizing microscope in conjunction with a Mettler FP-52 heating stage and a PL-DSC differential scanning calorimeter. The rate of heating or cooling was 10°C min^{-1}. The number average molecular mass and polydispersity of the polymers were characterized with a Waters GPC system (Waters 150C refractometer), relative to polystyrene standards. These are listed in table 1. Mass spectra were recorded on a GC-MS Shimadzu QP-5050 (EI, 70 eV).

Small angle X-ray scattering (SAXS) measurements were performed on the bending magnetic beamline BM2 at the European Synchrotron Radiation Facility (ESRF), Grenoble, France [12]; the incident energy was 16.2 keV. An indirect illumination CCD detector (Princeton Instruments) was used, at 27.5 cm from the sample. The scattering curve $I(q)$ was determined over a domain of q values ranging between 2×10^{-3} and 0.8 Å^{-1}. The powder samples were placed in a stainless steel sample holder closed by two mica windows of thickness 20 μm. The sequence glassy state–mesogenic phase–isotropic state was investigated with the samples mounted on a thermostatted block placed in the beam, in which the temperature was increased. The intensities were corrected for the detector response and the dark current signals, as well as for sample transmission and background scattering.

Depolarized light scattering experiments were performed on a standard set-up described elsewhere [8]. The light source was a He-Ne laser with wavelength 632.8 nm. The sample was oriented in a glass cell consisting of two glass plate substrates buffed with polyimide and an optical path of 5 μm (Linkam Scientific Instruments). The scattered light, I_{VH}, was analysed with a Glann–Thompson prism having an extinction ratio better than 10^{-7}.

Purification by column chromatography was carried out on 70–230 mesh Merck silica gel 60. (L)-(−)-Isoleucine,

Table 1. Comparative data and transition temperatures (T/°C)[a] of the chiral polyacrylates **P13** and **P14**. g = glassy state, S = smectic phase, N* = chiral nematic phase, I = isotropic liquid.

Polymer	M_n/g mol^{-1}	M_w/M_n	Yield/%	g		S		N*		I	[a]ΔH/kcal mru	$[\alpha]_D^{20}/°$ [d]
P13	21,200	1.60	57	•	37.3[b]	•	68.2			•	0.19	+7.0
P14	113,300	1.50	25	•	20.5[b]			•	63.1	•	[c]	+9.0

[a] Enthalpy in the phase transition from liquid state to a liquid crystalline state; mru = mole repeating unit. [b] Glass transition. [c] Value not determined. [d] [α]: 1.0 g in 100 ml CH_2Cl_2.

p-hydroxy methylbenzoate, 4-(*N*,*N*-dimethylamino)-pyridine (DMAP), *p*-toluenesulphonyl chloride, 1,3-dicyclohexylcarbodiimide (DCC), 2,2′-azobis(isobutyronitrile) (AIBN), diethylazodicarboxylate (DEAD) and triphenylphosphine (PPh$_3$) were purchased from Aldrich, and used as received unless otherwise specified. Dichloromethane (CH$_2$Cl$_2$) was distilled over calcium hydride under argon immediately before use. Analytical thin layer chromatography (TLC) was conducted on Merck aluminium plates with 0.2 mm of silica gel 60F-254. Anhydrous sodium sulphate was used to dry all organic extracts. Toluene was first heated at reflux over sodium and then distilled under argon. AIBN was freshly recrystallized from methanol.

2.1. *(2S,3S)-(+)-2-Chloro-3-methylpentanoic acid (2)*

Compound **2** was prepared according to conditions described by Koppenhoefer and co-workers [13 *a*]. Yield 67% of colourless oil. $[\alpha]^{20}_{D} = -1.44$ (neat). ^{1}H NMR (CDCl$_3$, 200 MHz): δ 0.93 (t, 3H, CH$_3$); 1.06 (d, 3H, CH$_3$); 1.25 (m, 1H, CH$_2$CH$_3$); 1.62 (m, 1H, CH$_2$CH$_3$); 2.15 (m, 1H, CHCH$_3$); 4.24 (d, 1H, CHCl, $J = 6.34$ Hz); 9.60 (board, 1H, CO$_2$H). ^{13}C NMR (CDCl$_3$, 50 MHz): δ 1085; 1586; 24.81; 38.77; 62.70; 175.24.

2.2. *(2S,3S)-(+)-2-Chloro-3-methyl-1-pentanol (3)* [13 *b*]

In a 2 l, three-necked, round-bottomed flask equipped with a mechanical stirrer, 50 ml dropping funnel, stopper and an efficient reflux condenser fitted with a calcium chloride drying tube, was placed lithium aluminium hydride (2.43 g, 0.064 mol); 110 ml of dry diethyl ether was added with caution. The slurry was cooled in an ice bath and a solution of compound **2** (8.00 g, 0.053 mol) in 40 ml of dry diethyl ether was added carefully with vigorous stirring over a 10 min period so that refluxing of the solvent was kept under control. After a total reaction time of 15 min, the drying tube was removed and 10 ml of water added dropwise with efficient stirring and cooling. The precipitate was dissolved by addition of 29 ml of 2N sulphuric acid. The layers were separated, and the aqueous layer extracted with three 100 ml portions of diethyl ether. The combined ether layers well washed with 50 ml of water, 50 ml of sodium carbonate solution and 50 ml of sodium bicarbonate solution, each aqueous layer being re-extracted with two 50 ml portions of diethyl ether. The combined ethereal layers were dried over sodium sulphate, and concentrated to give an oily residue. Fractional distillation at reduced pressure (i.e. b.p. 85°C at 22 mmHg) yielded 57% of colourless oil. $[\alpha]^{20}_{D} = -6.70$ (neat). ^{1}H NMR (CDCl$_3$, 200 MHz): δ 0.92 (t, 3H, CH$_3$, $J = 7.40$ Hz); 1.01 (d, 3H, CH$_3$, $J = 6.82$ Hz); 1.25 (m, 1H, CHHCH$_3$); 1.50 (m, 1H, CHHCH$_3$); 1.80 (m, 1H, CHCH$_3$); 2.20 (m, OH, board); 3.66 (dd, 1H, CHHOH, $^2J_{gem} = 12.10$, $^3J_{trans} = 7.74$ Hz); 3.77 (dd, CHHOH, $^2J_{gem} = 12.10$, $^3J_{cis} = 3.64$ Hz); 3.91 (ddd, 1H, CHCl, $^3J_{trans} = 7.70$ Hz, $^3J_{trans} = 5.62$, $^3J_{cis} = 3.60$ Hz). ^{13}C NMR (CDCl$_3$, 50 MHz): δ 10.9; 15.6; 24.7; 37.8; 64.4; 69.8; IR ν_{max}/cm^{-1} 3373; 2966; 2878; 1460; 1381; 1075; 1032; 814; 773 (nujol).

2.3. *4-Hydroxyphenyl benzoate (5)*

Compound **5** was synthesized following the procedure reported by Helgee and co-workers [14]. Yield 63%, m.p. 172°C. ^{1}H NMR (CDCl$_3$/DMSO, 200 MHz): δ 6.90 (dd, 4H, Ar); 7.52 (m, 3H, Ar); 8.10 (d, 2H, Ar). IR ν_{max}/cm^{-1}: 3368; 2928; 1515; 1463; 1377; 1242; 1105; 770; 722.

2.4. *(2S,3S)-(+)-4-[1-(2-Chloro-3-methyl)pentyloxy]-phenyl benzoate (6)*

A solution of DEAD (2.61 g, 15 mmol) and compound **3** (1.36 g, 10 mmol) in THF (5 ml) was added dropwise to a cold stirred solution of 4-hydroxyphenyl benzoate (2.14 g, 10 mmol), triphenylphosphine (3.93 g, 15 mmol) and THF (45 ml) during 1 h. The mixture was stirred at room temperature for 48 h and the solvent evaporated from the reaction mixture. The resulting oil was dissolved in ethyl acetate (25 ml) and four times this final volume was added of light petroleum. Triphenylphosphine oxide was precipitated; this was filtered off and the solution evaporated to dryness. The material obtained was purified by column chromatography on silica gel with hexane/ethyl acetate as eluent (9/1). Yield 1.85 g, (52%), white solid, $[\alpha]^{20}_{D} = +13$ (1.0, CH$_2$Cl$_2$). Anal: calc. for **6** C$_{19}$H$_{21}$O$_3$Cl (332.5 g mol^{-1}) C 68.67, H 6.32; found C 68.48, H 6.28%. ^{1}H NMR (CDCl$_3$, 200 MHz): δ 0.88 (t, 3H, CH$_3$, $J = 7.40$ Hz); 1.01 (d, 3H, CH$_3$, $J = 6.82$ Hz); 2.25 (m, 1H, CHHCH$_3$); 2.55 (m, 1H, CHHCH$_3$); 1.95 (m, 1H, CHCH$_3$); 4.15 (m, 3H, CH$_2$O, CHCl); 6.94 (d, 2H, Ar, $J = 9.13$ Hz); 7.12 (d, 2H, Ar, $J = 8.96$ Hz); 7.50 (m, 2H, Ar); 7.60 (m, 1H, Ar); 8.20 (d, 2H, Ar). ^{13}C NMR (CDCl$_3$, 50 MHz): δ 11.5; 16.1; 24.5; 38.1; 64.8; 70.3; 115.4; 122.5; 128.5; 129.5; 130.1; 133.5; 144.8; 156.0; 165.4. CG/MS (EI, 70 eV): 334 (M$^+$ + 2, 3%); 332 (M$^+$, 9%); 214 (3%); 105 (100%); 77 (51%); 51 (17%); 41 (16%).

2.5. *(2S,3S)-(+)-4-[1-(2-Chloro-3-methyl)pentyloxy]-phenol (7)*

To 1.34 g (4.0 mmol) of compound **6** in an ethanol/water mixture (30 ml), 0.26 g (4.8 mmol) of potassium hydroxide was added, and the mixture stirred overnight at room temperature. The ethanol was evaporated and the product extracted with diethyl ether; the solution was washed with water (2 × 25 ml), dried over Na$_2$SO$_4$ and purified on silica gel using ethyl acetate/hexane

(1/9) to yield 0.66 g (73%) $[\alpha]_D^{20} = +16$ (1.0; CH_2Cl_2), m.p. 60°C. ^1H NMR ($CDCl_3$, 200 MHz): δ 0.87 (t, 3H, CH_3, $J = 7.40$ Hz); 0.99 (d, 3H, CH_3, $J = 6.82$ Hz); 4.02 (m, 3H, $OC\underline{H}_2$, $C\underline{H}Cl$); 5.10 (broad, 1H, OH); 6.70 (m, 4H, Ar). ^{13}C NMR ($CDCl_3$, 50 MHz): δ 11.5; 16.1; 24.5; 38.1; 65.2; 70.8; 116.1; 116.2; 150.0; 152.5. IR ν_{max}/cm^{-1} 3363; 2965; 2877; 1604; 1455; 1511; 1229 (nujol). CG/MS (EI, 70 eV): 230 ($M^+ + 2$, 5%); 228 (M^+, 15%); 123 (3%); 110 (100%); 93 (5%); 81 (22%); 65 (13%); 55 (29%); 41 (33%).

2.6. *4-[(4-Propenoyloxy)undecyloxy]benzoic acid (8)*

Compound **8** was synthesized according to ref. [15]. White solid (92%), m.p. 94°C. IR ν_{max}/cm^{-1} 3080–2700; 2929; 2853; 1718; 1685; 1605; 1464; 1250; 1177; 1037; 854; 772 (KBr). ^1H NMR ($CDCl_3$, 200 MHz): δ 1.34 (m, 14H, CH_2); 1.72 (m, 4H, CH_2); 4.10 (m, 4H, CH_2O); 5.80 (dd, 1H, $CH{=}CH_2$); 6.15 (dd, 1H, $CH{=}CH_2$); 6.40 (dd, 1H, $CH{=}CH_2$); 6.90 (d, 2H, $J = 9.0$ Hz, Ar); 8.03 (d, 2H, $J = 8.8$ Hz, Ar).

2.7. *4-[(4-Propenoyloxy)butyloxy]benzoic acid (11)*

Compound **11** was prepared according to ref. [16]. White solid (61%), m.p. 122°C. IR ν_{max}/cm^{-1} 3100–2700; 2928; 2853; 1743; 1670; 1607; 1463; 1377; 1294; 1254; 1172; 960; 851; 722 (nujol). ^1H NMR ($CDCl_3$, 200 MHz): δ 1.78 (m, 4H, CH_2); 4.11 (m, 2H, CH_2O); 4.21 (s, 2H, CH_2O); 5.75 (dd, 1H, $CH{=}CH_2$); 6.05 (dd, 1H, $CH{=}CH_2$); 6.35 (dd, 1H, $CH{=}CH_2$); 6.85 (d, 2H, $J = 8.0$ Hz, Ar); 8.0 (d, 2H, $J = 8.0$ Hz, Ar).

2.8. *(2S,3S)-(+)-4-[1-(2-Chloro-3-methyl)pentyloxy]-phenyl 4[1-(propenoyloxy)undecyloxy]-benzoate ($\mathbf{M_9}$)*

The monomers $\mathbf{M_9}$ and $\mathbf{M_{12}}$ were synthesized according to ref. [17]. Compounds **7** (0.88 g, 3.8 mmol) and **8** (1.02 g, 3.8 mmol), were added to dry CH_2Cl_2 (30 ml) under argon and the solution was stirred at room temperature for 10 min. DCC (0.80 g, 3.9 mmol) and DMAP (47 mg, 0.39 mmol) were then added, and the solution was stirred for 24 h at room temperature. The solution was filtered and the solvent evaporated. The crude product was purified by column chromatography (silica gel, diethyl ether/hexane = 1/9) to yield 1.27 g (57%) of $\mathbf{M_9}$ as a white solid; m.p. 38°C, $[\alpha]_D^{20} = +7.0$ (1.0; CH_2Cl_2). Anal: calc. for $\mathbf{M_9}$ $C_{32}H_{44}O_6$ (524 g mol^{-1}) C 73.28; H 8.39; found C 73.08, H 8.47%. ^1H NMR ($CDCl_3$, 200 MHz): δ 0.92 (t, 3H, CH_3); 1.21 (d, 3H, CH_3); 1.50 (m, 20H, (CH_2), CH_2CH_3); 1.95 (m, 1H, $C\underline{H}CH_3$); 4.05 (m, 7H, $3CH_2O$, $C\underline{H}Cl$); 5.75 (dd, 1H, $CH{=}CH_2$, $^2J_{gem} = 1.60$, $^3J_{cis} = 10.20$ Hz); 6.05 (dd, 1H, $CH{=}CH_2$, $^3J_{cis} = 10.20$, $^3J_{trans} = 17.10$); 6.33 (dd, 1H, $CH{=}CH_2$, $^2J_{gem} = 1.80$, $^3J_{trans} = 17.20$ Hz); 6.90 (m, 4H, Ar); 7.05 (d, 2H, Ar, $J = 8.8$ Hz); 8.00 (d, 2H, Ar, $J = 8.6$ Hz). ^{13}C NMR ($CDCl_3$, 50 MHz): δ 11.5; 16.0; 24.5; 25.9; 28.6; 29.1; 29.2; 29.3; 29.4; 29.6; 38.0; 64.6; 64.8; 68.5; 70.3; 114.2; 115.4; 121.5; 122.6; 128.6; 130.3; 132.1; 144.9; 155.8; 163.4; 165.1; 166.2. IR ν_{max}/cm^{-1} 2923; 2859; 1729; 1607; 1511; 1462; 1377; 1259; 1192; 1165; 1057; 795; 716 (nujol).

2.9. *(2S,3S)-(+)-4-[1-(2-Chloro-3-methyl)pentyloxy]-phenyl 4[1-(propenoyloxy)butyloxy]-benzoate ($\mathbf{M_{12}}$)*

This compound was synthesized according to the procedure described above. Yield 0.56 g (74%) after column chromatography (silica gel, diethyl ether/hexane = 1/9) as a white solid, m.p. 40°C, $[\alpha]_D^{20} = +10.0$ (1.0; CH_2Cl_2). ^1H NMR ($CDCl_3$, 200 MHz): δ 0.94 (t, 3H, CH_3); 1.07 (d, 3H, CH_3); 1.25 (m, 1H, $C\underline{H}HCH_3$); 1.65 (m, 1H, $CH\underline{H}CH_3$); 2.00 (m, 5H, $C\underline{H}CH_3$, $(CH_2)_2$); 4.20 (m, 7H, $3CH_2O$, $C\underline{H}Cl$); 5.83 (dd, 1H, $CH{=}CH_2$, $^2J_{gem} = 1.46$, $^3J_{cis} = 10.30$ Hz); 6.12 (dd, 1H, $CH{=}CH_2$, $^3J_{cis} = 10.20$, $^3J_{trans} = 17.30$ Hz); 6.41 (dd, 1H, $CH{=}CH_2$, $^2J_{gem} = 1.46$, $^3J_{trans} = 17.30$ Hz); 7.02 (dd, 4H, Ar); 7.12 (d, 2H, Ar, $J = 9.20$ Hz); 8.14 (d, 2H, Ar, $J = 9.00$ Hz). ^{13}C NMR ($CDCl_3$, 50 MHz): δ 11.5; 16.0; 24.4; 25.3; 25.7; 38.0; 64.0; 64.5; 67.5; 70.2; 114.1; 115.3; 121.7; 122.5; 128.3; 130.6; 132.1; 144.8; 155.8; 163.1; 163.1; 165.1; 166.1. IR ν_{max}/cm^{-1} 2923; 2854; 1725; 1605; 1511; 1462; 1377; 1279; 1195; 1070; 963 (nujol).

2.10. *Polymerization*

All the polymerization reactions were carried out in toluene solution at 70°C using the initiator 2,2′-azobis(isobutyronitrile) AIBN (5 wt%). The yields were 60–90% based on total monomer added to the reaction. All reaction mixtures were heated under reflux for 72 h and, after cooling, were precipitated from cold methanol. The precipitates were purified by reprecipitation with cold methanol from toluene solution and dried in vacuum. The purity of homopolymers was checked by ^1H NMR. $\mathbf{P_{13}}$: yield 57%, $[\alpha]_D^{20}$ + 7.0 (1.0; CH_2Cl_2), $\mathbf{P_{14}}$: yield 25%, $[\alpha]_D^{20}$ + 9.0 (1.0; CH_2Cl_2).

3. Results and discussion

3.1. *Synthesis of (2S,3S)-(+)-4-[1-(2-chloro-3-methyl)-pentyloxy]phenol (7)*

The synthetic approach for the synthesis of chiral precursor **7** is outlined in schemes 1 and 2. The amino acid, L-isoleucine (**1**), was transformed into chiral intermediate **2** under diazotization conditions ($NaNO_2$/HCl) in 67% yield. The chiral α-aminoacids are important precursors for the synthesis of small organic molecules with high optical purity. Chiral halohydrins, oxiranes and alcohol are the most common products from diazotization

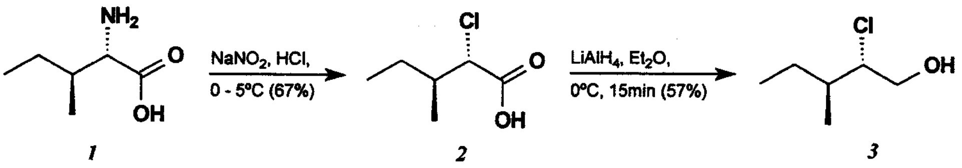

Scheme 1.

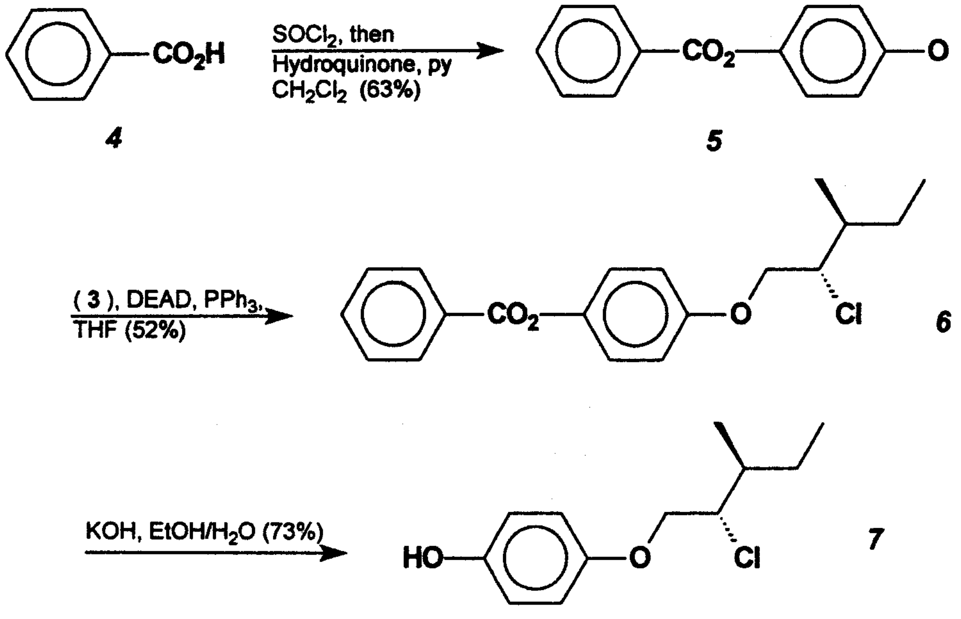

Scheme 2.

reactions of α-aminoacids. The next step in scheme 1 was the time-controlled lithium aluminium hydride reduction procedure developed by Koppenhoefer and co-workers [13] giving the chiral 2-chloroalcohol **3** with a 57% yield; this is a useful starting material for the synthesis of chiral liquid crystal assemblies. This procedure was used to prevent hydrogenolysis of the chlorine–carbon bond [18].

The stereochemical outcome of chlorination by diazonium salt reaction was confirmed by proton NMR analysis. From the ^{1}H NMR spectrum we observed a signal at 4.2 ppm as a doublet with $J_{H_\alpha H_\beta} = 6.34$ Hz. No other signal was detected in this spectral region, indicating a diastereomeric excess of $>95\%$. Nucleophilic substitution takes place with retention of the configuration [19–21] by means of double configuration inversion of an unstable α-lactone (figure 2).

Synthesis of the key intermediate **7** was achieved by the Mitsunobu reaction [22] starting from hydroquinone monobenzoate **5** [14] and the chiral chloroalcohol **3**. Compound **5** was synthesized in 63% yield by conversion of **4** into the acyl derivative followed by reaction with hydroquinone in pyridine. The corresponding diester was obtained in a yield of 16% as a by-product. We investigated the best condition for the Mitsunobu reaction to give compound **6** in 52% yield and $[\alpha]_D^{20} = +13.0$ (1, CH_2Cl_2). Basic hydrolysis yielded (2*S*,3*S*)-(+)-4-[1-(2-chloro-3-methyl)pentyloxy]phenol (**7**) in 73% yield and $[\alpha]_D^{20} = +16.0$ (1, CH_2Cl_2).

The reaction conditions for synthesis of compound **6** under Mitsunobu coupling were investigated. The choice of solvent is critical owing to the low solubility of compound **5**. In CH_2Cl_2, the reaction yields the desired product **6**, but all attempts to repeat that reaction either gave poor yields (15–25% yield) or failed [23]. We found that the best conditions were those involving THF as solvent. THF solutions of **3** and diethyl azodicarboxylate were added over 1 h to the solution of **5** and PPh_3 at 0°C. The temperature was then allowed to rise to 25°C over 48 h.

The stereochemistry of intermediate **6** was established unequivocally by single crystal X-ray structure determination (figure 3), showing that the nucleophilic displacement of chiral diazonium salts in scheme 1 proceeds with overall retention of configuration. To the best of our knowledge this is the first example in which a chloro derivative has been synthesized from a chiral aminoacid and its crystalline structure determined.

The Flack [24] parameter should be 0 (within 3 ESDs) if the absolute structure is the one refined. In this case

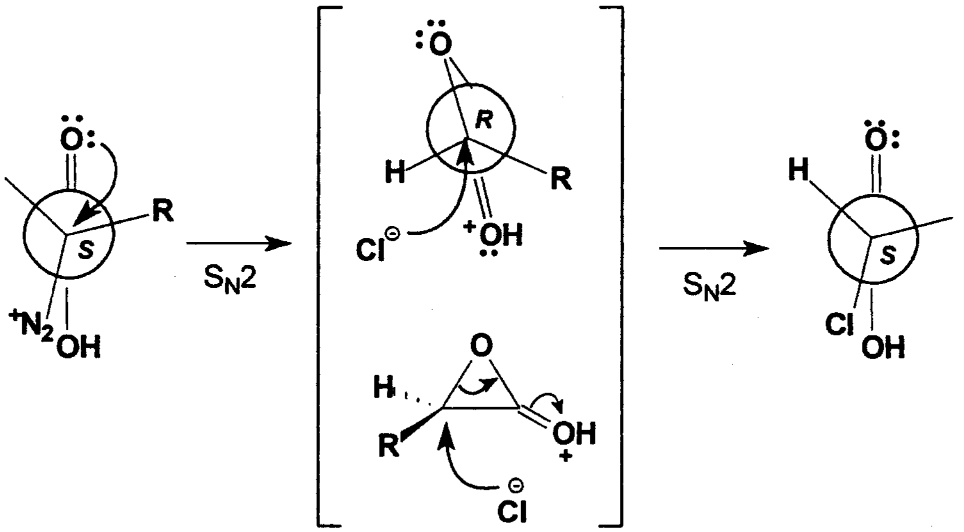

Figure 2. Mechanistic representation of the first and second steps in the nucleophilic displacement of chiral diazonium salts through an unstable intermediate α-lactone. The starting material has *S* configuration at the C-2 centre. Internal nucleophilic attack from the neighbouring oxygen yields an unstable intermediate with inverted configuration at the C-2 centre. The second nucleophilic attack from an external chlorine atom opens the three-member ring and gives the product with inverted inversion at the C-2 centre. The net result is that the reaction proceeds with overall retention of configuration.

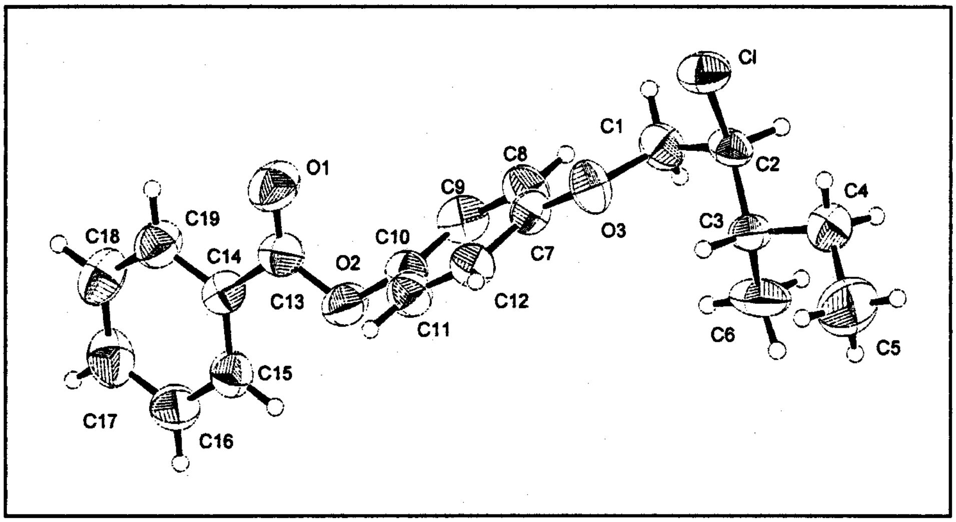

Figure 3. Molecular structure of (2*S*,3*S*)-(+)-4-[1-(2-chloro-3-methyl)pentyloxy]phenyl benzoate (**6**). Perspective view and atom labelling; thermal ellipsoids are given at the 50% probability level.

it is 0.12(12), which means that the configuration shown in the picture corresponds, without ambiguity, to the absolute configuration.

Table 2 shows the crystal data and structure refinement for compound **6**. Atomic coordinates and equivalent isotropic displacement parameters are shown in table 3. Tables 4 and 5 list the bond lengths and bond angles for **6**, respectively.

From the tables, we see that both phenyl rings are planar, to within experimental accuracy, as can be seen by the σ_{av} {defined as $[(\Sigma_i d_i^2)/N - 3]^{1/2}$, where d_i is the deviation of the atom from the best least squares plane and N the number of atoms forming the plane} values of 3.3×10^{-3} and 4.5×10^{-3} for the C7 to C12 and C14 to C19 planes, respectively. The phenyl rings make a dihedral angle of 75.9(1)°. The torsion angle for rotation about the C1 and C2 atoms of aliphatic tail indicates that *gauche* conformation is adopted. The more stable *anti* conformation is not seen for C1 and C2 atoms in solid crystalline. However the *anti* conformation is observed in the torsion angle for rotation about the C2 and C3 atoms, so that an antiperiplanar arrangement between C1 and C6 atoms in figure 3 is evidence for the stereochemical integrity of the diazotization reaction.

Table 2. Crystal data and structure refinement of compound **6**.

Empirical formula	$C_{19}H_{21}ClO_3$
Formula weight	332.81
Temperature	293 K
Wavelength	0.71073 Å
Crystal system	orthorhombic
Space group	$P2_12_12_1$
a/Å	5.7890(9)
b/Å	9.096(1)
c/Å	33.500(4)
U/Å	1764.0(4)
Z	4
D_c/g cm^{-3}	1.253
Absorption coefficient/mm^{-1}	0.228
F(000)	704
Crystal size/mm^3	0.20 × 0.20 × 0.15
θ range for data collection/°	1.22 to 27.97
Limiting indices	$-1 \leqslant h \leqslant 7$, $-12 \leqslant k \leqslant 0$, $0 \leqslant l \leqslant 44$
Reflections collected	2935
Independent reflections	2858 [$R_{int} = 0.0182$]
ψ-scan absorption correction	
Max., min. transmission factors	0.9666, 0.9554
Refinement method	Full-matrix least-squares on F^2
Data/restraints/parameters	2858/0/210
Goodness-of-fit on F^2	0.984
Final R indices [$I > 2\sigma(I)$]	$R1 = 0.0332$, $wR2 = 0.0719$
Largest diff. peak and hole$^{\rho}$ (e Å^{-3})	0.177 and −0.252

Table 3. Atomic coordinates (× 10^4) and equivalent isotropic displacement parameters (Å^2 × 10^3) for nnn. U_{eq} is defined as one third of the trace of the orthogonalized U_{ij} tensor.

Atom	X	Y	Z	U_{eq}
Cl	1596(2)	7189(1)	3767(1)	64(1)
O(1)	7613(6)	7470(4)	1386(1)	76(1)
O(2)	10144(6)	8820(3)	1729(1)	60(1)
O(3)	5349(6)	8013(3)	3136(1)	58(1)
C(1)	3684(8)	9077(5)	3268(1)	57(1)
C(2)	3250(8)	8863(4)	3705(1)	48(1)
C(3)	5384(8)	8831(4)	3967(1)	49(1)
C(4)	4705(10)	8858(6)	4409(1)	69(2)
C(5)	6717(11)	8625(6)	4696(2)	103(2)
C(6)	6940(9)	10134(5)	3868(2)	77(2)
C(7)	6421(9)	8262(4)	2779(1)	47(1)
C(8)	5744(8)	9303(4)	2504(1)	58(1)
C(9)	6967(10)	9457(5)	2151(1)	60(1)
C(10)	8824(9)	8596(5)	2080(1)	51(1)
C(11)	9531(9)	7546(4)	2353(1)	58(1)
C(12)	8326(8)	7395(4)	2704(1)	52(1)
C(13)	9311(9)	8223(4)	1390(2)	53(1)
C(14)	10697(9)	8627(4)	1036(1)	46(1)
C(15)	12738(9)	9393(5)	1061(1)	57(1)
C(16)	13998(10)	9721(5)	720(2)	67(2)
C(17)	13176(11)	9287(5)	353(2)	74(2)
C(18)	11147(11)	8514(5)	324(2)	71(2)
C(19)	9912(10)	8178(5)	663(1)	63(1)

Table 4. Bond lengths (Å) for non-hydrogen atoms for structure **6** in scheme 2.

Cl–C(2)	1.81094)
O(1)–C(13)	1.197(5)
O(2)–C(13)	1.350(5)
O(2)–C(10)	1.417(5)
O(3)–C(7)	1.367(5)
O(3)–C(1)	1.435(5)
C(1)–C(2)	1.498(5)
C(2)–C(3)	1.517(6)
C(3)–C(6)	1.525(6)
C(3)–C(4)	1.533(6)
C(4)–C(5)	1.524(6)
C(7)–C(8)	1.377(5)
C(7)–C(12)	1.379(6)
C(8)–C(9)	1.387(6)
C(9)–C(10)	1.351(6)
C(10)–C(11)	1.383(6)
C(11)–C(12)	1.374(6)
C(13)–C(14)	1.479(6)
C(14)–C(15)	1.375(6)
C(14)–C(19)	1.389(6)
C(15)–C(16)	1.387(6)
C(16)–C(17)	1.378(6)
C(17)–C(18)	1.373(7)
C(18)–C(19)	1.378(6)

Table 5. Bond angles (°) for non-hydrogen atoms for structure **6** in scheme 2.

C(13)–O(2)–C(10)	116.6(4)
C(7)–O(3)–C(1)	117.5(3)
O(3)–C(1)–C(2)	109.0(3)
C(1)–C(2)–C(3)	115.6(4)
C(1)–C(2)–Cl	108.1(3)
C(3)–C(2)–Cl	110.4(3)
C(2)–C(3)–C(6)	109.9(3)
C(2)–C(3)–C(4)	110.6(4)
C(6)–C(3)–C(4)	110.5(4)
C(5)–C(4)–C(3)	114.2(4)
O(3)–C(7)–C(8)	124.7(4)
O(3)–C(7)–C(12)	115.4(4)
C(8)–C(7)–C(12)	119.9(4)
C(7)–C(8)–C(9)	119.6(4)
C(10)–C(9)–C(8)	119.8(4)
C(9)–C(10)–C(11)	121.3(5)
C(9)–C(10)–O(2)	119.4(4)
C(11)–C(10)–O(2)	119.2(4)
C(12)–C(11)–C(10)	118.9(4)
C(11)–C(12)–C(7)	120.4(4)
O(1)–C(13)–O(2)	122.1(5)
O(1)–C(13)–C(14)	125.4(5)
O(2)–C(13)–C(14)	112.4(4)
C(15)–C(14)–C(19)	119.1(5)
C(15)–C(14)–C(13)	122.9(4)
C(19)–C(14)–C(13)	118.0(4)
C(14)–C(15)–C(16)	120.6(4)
C(17)–C(16)–C(15)	119.5(5)
C(18)–C(17)–C(16)	120.4(5)
C(17)–C(18)–C(19)	119.9(5)
C(18)–C(19)–C(14)	120.4(5)

3.2. *Synthesis of chiral monomers* *M*$_9$ *and* *M*$_{12}$ *containing eleven and four carbon atoms in the spacer group*

Schemes 3 and 4 describe the synthesis of the chiral monomers **M**$_9$ and **M**$_{12}$. The 4-(11-hydroxyundecyloxy)-benzoic acid was prepared by alkylation [25] with methyl *p*-hydroxybenzoate and 11-bromo-1-undecanol (K$_2$CO$_3$, CH$_3$CN) with 76% yield. Basic hydrolysis followed by addition of concentrated hydrochloric acid gave the acid derivative in 85% yield. Next, we synthesized the 4-[(4-propenoyloxy) undecyloxy] benzoic acid (**8**) in 92% yield [15, 8]. The final step in scheme 3 is the esterification reaction using DCC as dehydrating agent, DMAP as catalyst [17], and phenol **7**. The target molecule of (2*S*,3*S*)-(+)-4-[1-(2-chloro-3-methyl)-pentyloxy] phenyl 4-[1-(propenoyloxy) undecyloxy]-benzoate (**M**$_9$) was obtained with 57% yield.

The chiral monomer **M**$_{12}$ was prepared as outlined in scheme 4. The key intermediate 4-[(4-propenoyloxy)-butyloxy] benzoic acid (**11**) was prepared by the method described in ref. [24], with a slightly different first step. Instead of 4-bromobutyl acetate we used 4-chlorobutyl acetate, obtained from the quantitative ring-opening reaction of THF with acetylchloride and zinc chloride (catalyst) under reflux. The final step of the synthetic scheme is the esterification reaction providing the chiral monomer ester **M**$_{12}$ that was prepared from compounds **11** and **7** using DCC in CH$_2$Cl$_2$ containing a catalytic amount of DMAP [17]. The monomers **M**$_9$ and **M**$_{12}$ were isolated by silica gel column chromatography. The purified monomers were characterized by spectroscopic methods, and satisfactory analytical data were obtained (see § 2).

3.3. *Polymerization*

The monomers were submitted to free radical polymerization with 2,2′-azobis(isobutyronitrile) (AIBN, 5 wt%) as the radical initiator in toluene to give the chiral polyacrylates **P**$_{13}$ and **P**$_{14}$ (scheme 5). The low yield of **P**$_{14}$ (table 1) is due to several precipitations in cold methanol from toluene solution until no signal of olefinic protons in NMR spectrum was observed.

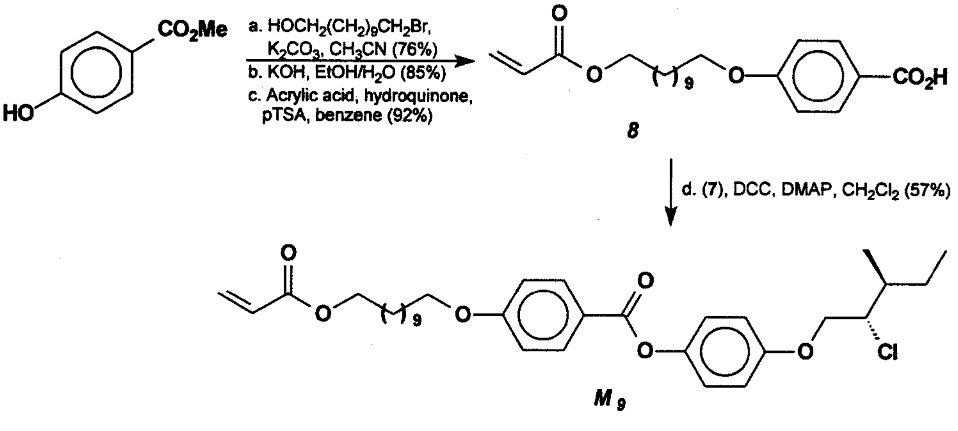

Scheme 3.

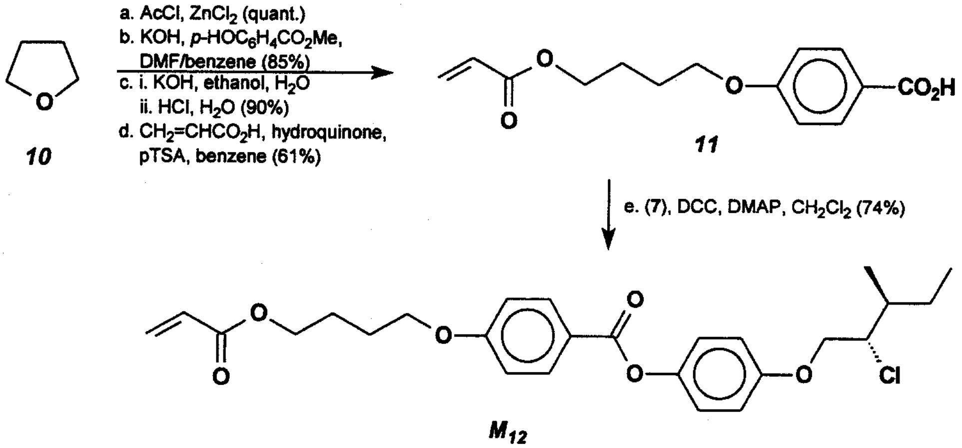

Scheme 4.

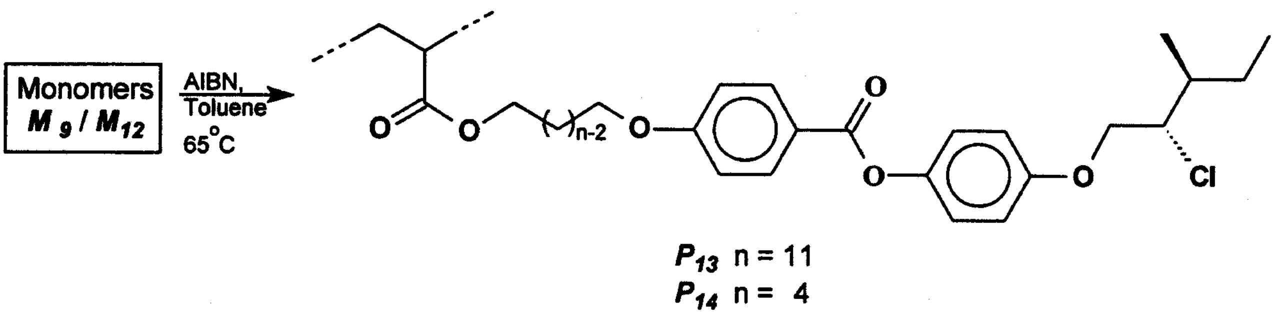

Scheme 5.

3.4. *Crystal structure determination*

Suitable crystals of (2*S*,3*S*)-(+)-4-[1-(2-chloro-3-methyl)-pentyloxy]phenyl benzoate (**6**) were grown at room temperature from ethyl acetate solution by slow evaporation. Data were collected on a CAD-4 Mach 3 Enraf Nonius diffractometer, in the $\omega/2\theta$ scan mode with ω scan width = 0.80 + 0.35 tan θ, using graphite monochromated MoK$_\alpha$ radiation. Data were corrected for Lorentz, polarization and absorption effects. The structure was solved by the standard heavy atom Patterson method, followed by normal difference Fourier techniques. H-atoms were located on stereochemical grounds, and refined with fixed geometry, each riding on a carrier atom, with an isotropic displacement parameter amounting to 1.5 (for methyl H atoms) or 1.2 (for the other H atoms) times the value of the equivalent isotropic displacement parameter of the atom to which they are attached. A summary of crystallographic parameters is presented in table 2. The final atomic coordinates and equivalent isotropic thermal parameters are listed in table 3. Tables 4 and 5 display bond lengths and bond angles for non-hydrogen atoms. The programs used were SHELXS-86 [26], SHELXL-97 [27], ZORTEP [28] and PARST [29].

3.5. *Mesomorphic properties of the chiral homopolymers* P^{13} *and* P^{14}

The mesomorphic and thermal behaviours of the homopolymers investigated by differential scanning calorimetry (DSC) and optical microscopy are summarized in table 1. The polymer with eleven methylene units in the spacer group, **P13**, has the smaller number average molecular weight, M_n. The molecular weight distributions M_w/M_n are similar for both **P13** and **P14**.

The DSC thermograms of the polyacrylate **P13** can be seen in figure 4. They show two endothermic peaks

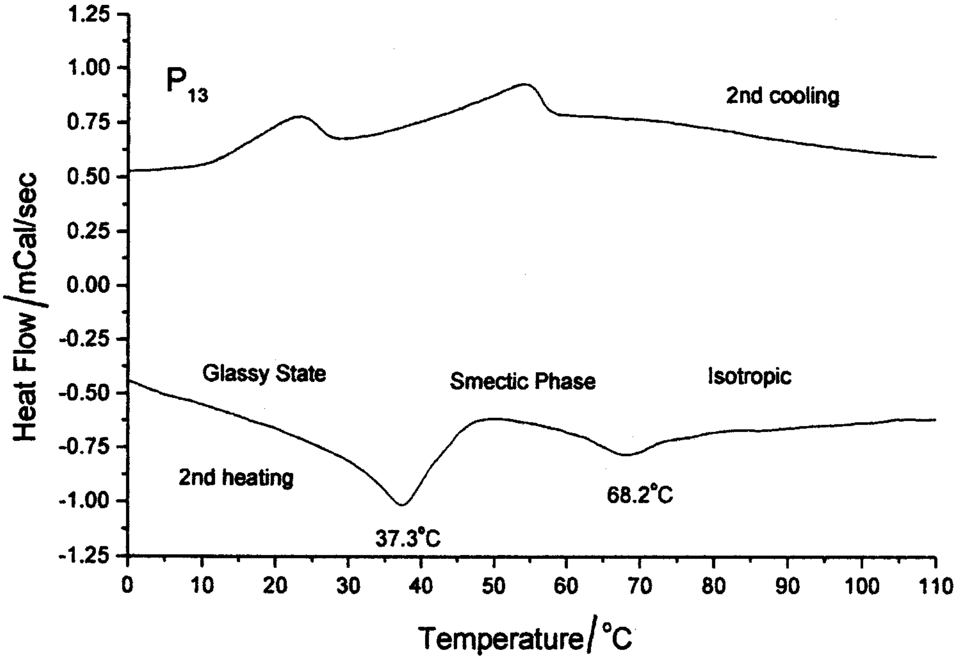

Figure 4. DSC thermogram of the polyacrylate **P13** as a function of temperature for the second heating and cooling cycles. Scan rates of 10°C min^{-1} (1 cal = 4.18 J).

at 37.3 and 68.2°C during the second heating scans, associated with the transition from the glassy state to the mesophase for the first peak, and from the mesophase to the isotropic liquid for the second peak. The temperature range for the mesophase is 30.9°C. The nature of the mesophase was tentatively assigned as smectic for **P13** with a blurred Schlieren texture, as observed by optical microscopy.

The DSC thermogram for **P14** has the same appearance as that **P13**, and exhibits two small peaks at 20.5 and 61.5°C related to the transitions glassy state → mesophase → isotropic state, respectively. The range of temperature for the mesophase is 41.0°C; it was assigned as nematic by optical microscopy. Smectic and nematic order are favoured after polymerization for both **P13** and **P14**; they do not crystallize upon cooling, but instead vitrify to liquid crystalline glasses. The phase behaviour of the monomers was also investigated, but none possesses a stable liquid crystal phase above the melting point.

3.6. *Small angle X-ray scattering*

Attempts to align the polymer samples by cooling them from the isotropic phase in a magnetic field of 0.5 T over a period of a few hours proved unsuccessful, probably due to their high viscosity. Temperature-dependent SAXS profiles of samples of **P13** and **P14** are given in figures 5 and 6, respectively.

The results obtained by analysis of the SAXS profiles are summarized in table 6. The glassy state → smectic phase transition of sample **P13** can be observed in figure 5, from the splitting of the two peaks, at $q = 0.202$ and $0.330\,\text{Å}^{-1}$, at 22°C, into the two peaks at $q = 0.178$ and $0.356\,\text{Å}^{-1}$, at 38°C. The well defined inner peaks, giving d-spacings in the range 35.30 to 34.56 Å on increasing the temperature between 38 and 60°C (see table 6), correspond to the smectic layer spacing of molecular orientational order [30]. Their reflections consisted of a circle with nearly uniform intensity, indicating

Table 6. Layer spacing, d, normalized intensity, $I(q)/I(q)^{\max}$, and mean mesogenic fluctuation amplitude, $\sqrt{\Delta x^2}/L$, from small angle X-ray scattering.

	P13			**P14**
$T/°\text{C}$	$d/\text{Å}$	$I(q)/I(q)^{\max}$	$\sqrt{\Delta x^2}/L$[a]	$d/\text{Å}$
22	31.12	0.10	—	27.04
38	35.30	1.0	0.0	—
42	35.08	0.92	0.07	27.32
50	35.84	0.34	0.14	27.61
60	34.56	0.08	0.19	—

[a] L (35.18 Å) is calculated from the monomer repeat unit in their fully extended conformation [35].

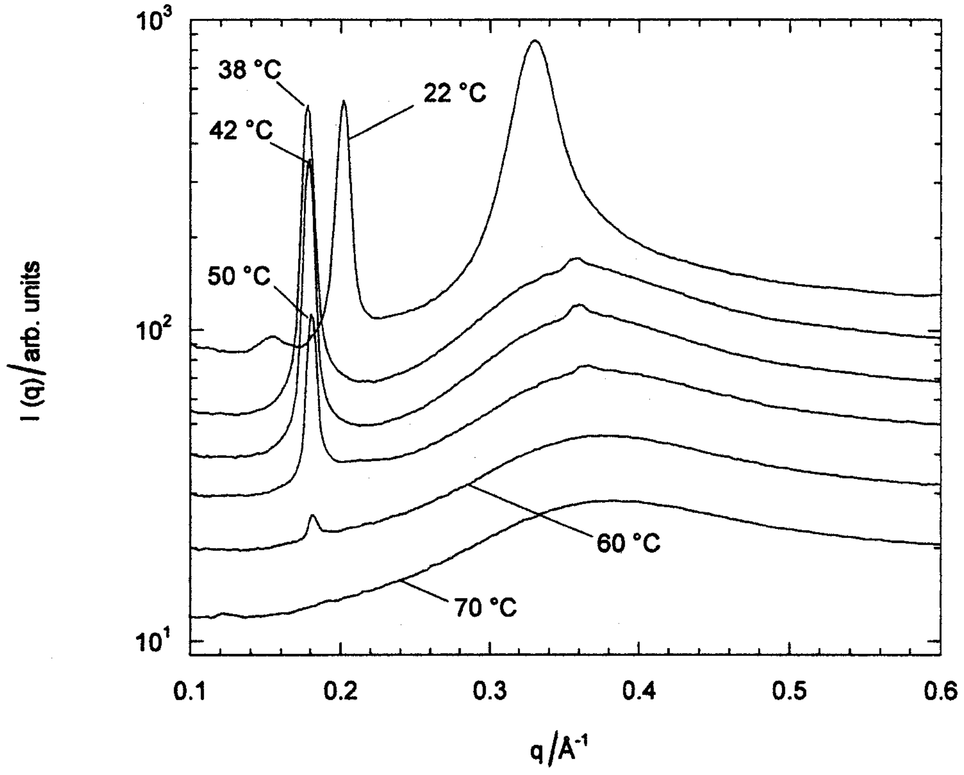

Figure 5. Small angle X-ray scattering profiles of the polyacrylate **P13** as a function of temperature for a heating cycle.

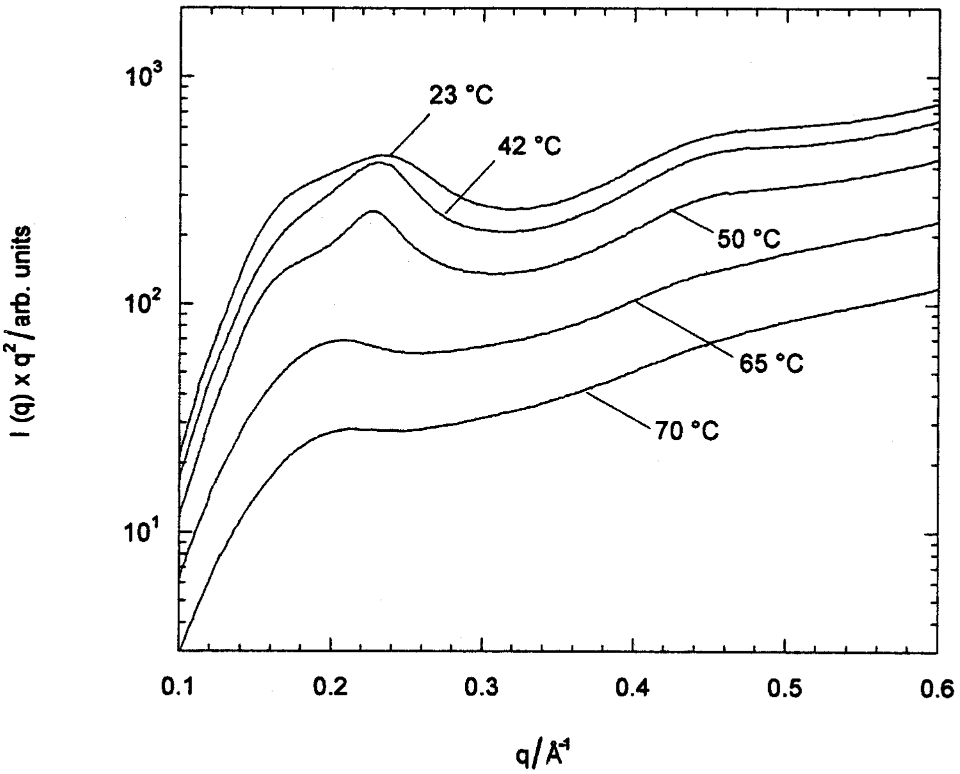

Figure 6. Small angle X-ray scattering profiles of the polyacrylate **P14** as a function of temperature for a heating cycle.

that smectic layers were formed with no preferred direction. The liquid-like intermesogenic organization within the layers, which appears as a diffuse outer peak (*c*. 1.2 Å^{-1}) in the X-ray profile of samples displaying disordered smectic phases [31], could not be observed owing to the limited q range utilized in this work. The second order Bragg reflections are also just visible for the temperatures 38, 42 and 50°C, at $q \approx 0.36$ Å^{-1}, superimposed on a diffuse peak. Two sharp signals with Bragg spacings in the ratio 1:2 in the low angle region are typical of smectic phases.

The broad diffuse scattering peak, which appears as another secondary maximum and can be observed also in the isotropic phase, may be attributed to the underlying polymer backbone. In the smectic phase, it is known that the main chains can preferentially occupy the space between the mesogenic layers [32] if the spacers are flexible [33].

In addition, the intensity of the low angle peak increases with increasing temperature, from 22 to 38°C (see table 6). As the temperature increases beyond 42°C, however, their intensity begins to decrease. Since this intensity depends also on the order [34], the increase suggests a higher degree of order of the smectic layers, due to the increasing mobility of the main polymer chain. The subsequent intensity decrease indicates that for higher temperatures, the backbone motion begins to reduce the number of regions with ordered structures inside the sample [34].

The fully extended length of a side chain mesogenic unit of **P13**, L, was estimated by means of semi-empirical calculations using the AM1 Hamiltonian [35], to be 35.18 Å. In the glassy state (22°C), the inner peak corresponds to a layer of 31.1 Å. This difference may be related to the mesogenic units, which are poorly stiffened between the polymer backbones. Because the ratio d/L is ~1 in the mesophase, between 38 and 60°C, the smectic structure has monolayer character, i.e. SmA$_1$. As the layer spacing d becomes slightly smaller with increasing temperature, we interpret this effect as the result of a larger amplitude motion of the mesogenic units attached to the polymer backbone. Since d and L are known, the amplitude of vibration, Δx, at each temperature is given through the relation:

$$d^2 + \langle \Delta x^2 \rangle = L^2. \tag{1}$$

The calculated values of Δx were used to estimate the mean mesogenic fluctuation amplitude, $\sqrt{\Delta x^2}/L$, as a function of the temperature. These are listed in table 6. According to these results, melting occurs only when the mean mesogenic fluctuation amplitude exceeds 0.19. This value is higher than the fraction ≈3.7%, that is typical for the melting of a number of metals [36], and reflects the stability of the smectic layers due to the presence of the polymer backbone.

The SAXS profiles of **P14** can be seen in figure 6, plotted in a Iq^2 vs. q representation, which reveals broad features in the scattering pattern. The profiles are typical of the nematic phase of side chain polymers, where only positional liquid-like short range order is present [37]. The small angle scattering response has a maximum that corresponds to the length of the repeat unit of the polymer, d. From the peak position an apparent side chain length could thus be obtained, also listed in table 6.

Thus, on changing the spacer from 11 methyl groups in the smectic sample **P13** to 4 in **P14**, the one-dimensional long range positional order is lost, which means that the smectic order develops more easily when the coupling between the mesogenic cores and the backbone weakens.

3.7. *Depolarized light scattering*

For this experiment the glass cell containing the sample was placed with the director **n**, related to the long range orientational order of the mesogenic side groups [38], perpendicular to the scattering plane. A reference sample, pentylcyanobiphenyl (5CB–Aldrich) was first investigated in the same way, in order to stabilize standard experimental conditions and to reproduce literature results [39]. To avoid unwanted scattering, the cell was always placed in an index matching bath (Decalin, Aldrich). The depolarized intensities, I_{VH}, were measured by heating the sample at a rate of 0.35°C min^{-1}, determined by the conditions of the equipment. The scattering behaviour observed for the **P13** sample as a function of temperature is shown in figure 7. The glassy →smectic, as well as the smectic →isotropic phase transitions, could be clearly detected, as indicated. The positions are in accordance with the values obtained by DSC analysis (see table 1 and figure 4).

As a rule, depolarized light scattered by a molecular system is related to the optical anisotropy of the molecule, ultimately related to molecular conformations. For the polyacrylates investigated in this work, the evolution of I_{VH} with temperature can be related to the orientational arrangement of the mesogenic moieties. The depolarized light scattered by the mesogenic segments is given by [40]:

$$I_{VH} = N\beta^2 n\langle \sin^2\theta \cos^2\theta \sin^2\varphi\rangle \qquad (2)$$

where N is the number of scattering particles in the scattering volume, β^2 is the optical anisotropy of the segment and n is the number of segments. θ and φ are the orientation angles of the symmetry axis of the segment in a laboratory-fixed frame. Since each segmental position with respect to φ is as likely as any other, and taking the scattering of all the segments in

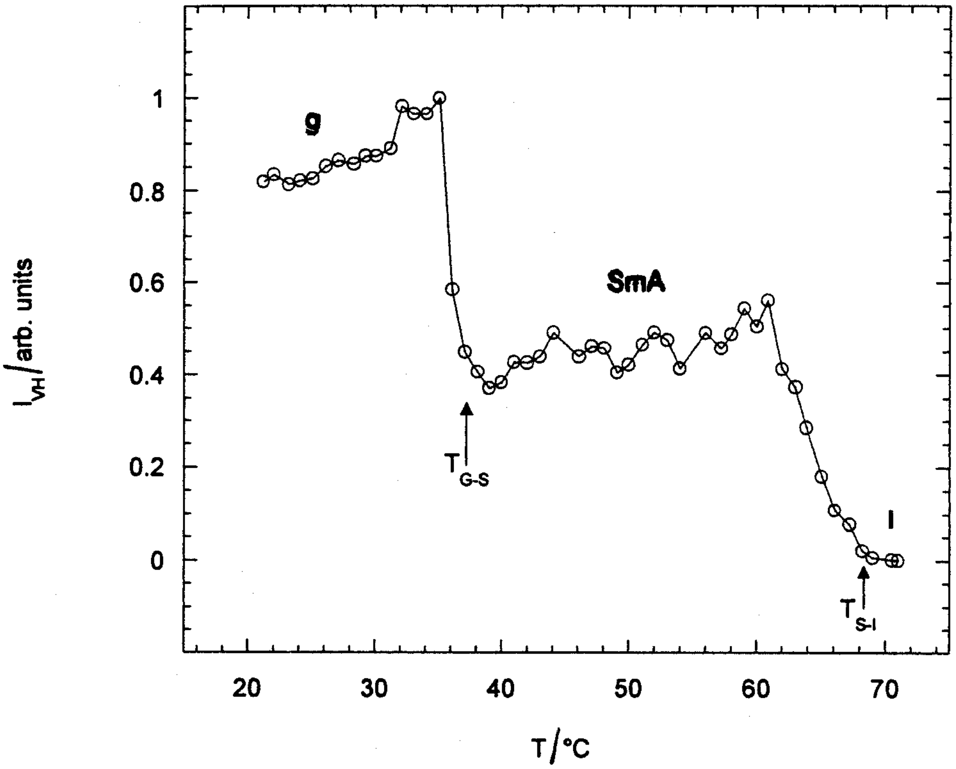

Figure 7. Depolarized light intensity, I_{VH}, scattered by the **P13** sample as a function of temperature for a heating cycle.

the polymer chain, equation (2) can be rewritten as:

$$I_{\mathrm{VH}} = N\langle\gamma^{2}\rangle\frac{1}{2}\langle\sin^{2} 2\theta\rangle \tag{3}$$

with $\langle\gamma^{2}\rangle$ the mean-squared optical anisotropy of the polymer. Thus changes in the positional orientation in the system can be detected by measuring I_{VH}. In this way $\langle\sin^{2} 2\theta\rangle$ can be defined as an order parameter for this polycrystalline system. To obtain $\langle\sin^{2} 2\theta\rangle$ for the smectic phase of **P13**, we relate the scattered light in the smectic I_{VHS} to that in the glassy state I_{VHG}, which is the more ordered state, and for which $\langle\sin^{2} 2\theta\rangle$ takes its maximum value:

$$\frac{I_{\mathrm{VHS}}}{I_{\mathrm{VHG}}} = \frac{N\langle\gamma^{2}\rangle\frac{1}{2}\langle\sin^{2} 2\theta\rangle}{N\langle\gamma^{2}\rangle\frac{1}{2}}. \tag{4}$$

Taking the mean value for I_{VHS} (between 40 and 60°C) and the maximum value for I_{VHG} (at 35°C) in figure 7, gives $\langle\sin^{2} 2\theta\rangle = 0.47$. This information can be used as a reference for the degree of order that can be achieved by the liquid crystalline polyacrylate **P13**. It is important to emphasize that this approach takes all the integrated depolarized scattered light into account. In order to obtain the absolute order parameter $\langle P_2\rangle$ by means of light scattering, the value of $\langle\gamma^{2}\rangle$ or $\langle P_2\rangle_{\mathrm{G}}$, the order parameter in the glassy state, must be known.

Furthermore, the relative increase of orientation with temperature observed between 40 and 60°C could be dominated by the effects of increasing chain mobility that favour the alignment of the smectic layers. A pretransitional effect can be seen at higher temperatures, just before reaching the isotropic phase. This may be caused by thermal fluctuations which affect the local orientation in the ordered domains. Similar behaviour is observed in the glassy state → smectic phase transition.

4. Conclusions

In this work new chiral side chain liquid crystalline polyacrylates **P13** and **P14** were synthesized and their mesomorphic behaviours investigated. The molecular structure of the polyacrylates has a substituted phenylbenzoate system as a core, a flexible spacer group having four or eleven methylenic units inserted between the core and polymerizable acrylate unit, and a chiral chain derived from L-isoleucine.

From L-isoleucine we synthesized a key intermediate (2*S*,3*S*)-(+)-4-[1-(2-chloro-3-methyl)pentyloxy]phenyl benzoate (**6**) by a Mitsunobu reaction; its stereochemistry was established unequivocally by single crystal X-ray analysis showing that the nucleophilic displacement of chiral diazonium salts proceeds with overall retention of configuration. The Flack parameter refined to 0.12(12) gave an accurate determination of the absolute configuration of the crystal structure of **6**. The intermediate **6** was hydrolysed under basic conditions to give the target phenol **7**. The esterification reaction between **7** and polymerizable *p*-substituted benzoic acids **8** and **11** gave the non-mesogenic monomers **M9** and **M12**. Polymerization (AIBN, 5 wt %) yielded the mesogenic polyacrylates **P13** and **P14**.

The chiral polyacrylates **P13** and **P14** showed the enantiotropic smectic A and nematic phase, respectively. A comparison of data obtained from thermal analysis and small angle X-ray scattering reveals that mesomorphic behaviour is dependent on both molecular mass and spacer length. Thus, we observed the chiral nematic phase for the polymer with higher molecular weight and shorter spacer group, and the smectic A phase for lower molecular weight and longer spacer group.

In addition, depolarized light scattering seems to be a promising technique for the investigation of the characteristic phase transition temperatures in the oriented samples, as well as to indicate the degree of order of the polymer chains in the mesophase.

Many thanks are due to Profs Ted R. Taylor and Hugo Gallardo (Universidade Federal de Santa Catarina-Brazil) for helpful discussions on the texture of the polyacrylates **P13** and **P14**, and to A. de Geyer, CEA, Grenoble, France, for preliminary X-ray measurements. A.A.M. and N.P.S. gratefully acknowledge the Brazilian Secretary for Science and Technology for funding under Grant No 620262/97-4-QEQ-PADCT-III-CNPq, and the agencies FAPESP-SP, FAPERGS-RS and Propesq-UFRGS. N.P.S. and F.V.P. acknowledge, respectively, a post-doctoral and a master fellowship from CAPES/Brazil. The authors are also grateful to the ESRF, Grenoble, France, for access to the CRG beamline BM2.

References

[1] Finkelmann, H., Ringsdorf, H., and Wendorff, J. H., 1978, *Makromol. Chem.*, **179,** 273.

[2] Hsu, C.-S., 1997, *Prog. polym. Sci.*, **22,** 829.

[3] MacArdle, C. B., 1989, *Side Chain Liquid Crystal Polymers* (London: Blackie).

[4] (*a*) Meyer, R. B., Lièbert, L., Strzelecki, L., and Keller, P., 1975, *J. Physique (Lett.)*, **36,** L69; (*b*) Meyer, R. B., 1977, *Mol. Cryst. liq. Cryst.*, **40,** 33.

[5] Clark, N. A., and Lagerwall, S. T., 1980, *Appl. Phys. Lett.*, **36,** 899.

[6] (*a*) Shibaev, V. P., Kozlovsky, M., Beresnev, L., Blinov, L., and Platè, N., 1984, *Polym. Bull.*, **12,** 299; (*b*) Shibaev, V. P., and Platè, N., 1985, *Pure appl. Chem.*, **57,** 1589.

[7] (*a*) Walba, D. M., Xiao, L., Keller, P., Shao, R., Link, D., and Clark, N., 1999, *Pure appl. Chem.*, **71,** 2117; (*b*) Busson, P., Ihre, H., Örtegren, J., Gedde, U. W., Hult, A., and Anderson, G., 2001,

Macromolecules, **34,** 1221; (*c*) Verrall, M., Beattie, D., Coates, D., Sage, I., and Lymer, K., 1996, *Ferroelectrics*, **181,** 327; (*d*) Baxter, B. C., and Gin, D. L., 1998, *Macromolecules*, **31,** 4419; (*e*) Scherowsky, G., Fichna, U., and Wolff, D., 1995, *Liq. Cryst.*, **19,** 621; (*f*) Fujishiro, K., and Lenz, R. W., 1992, *Liq. Cryst.*, **12,** 561; (*g*) Scherowsky, G., Schliwa, A., Springer, J., Kühnpast, K., and Trapp, W., 1989, *Liq. Cryst.*, **5,** 1281; (*h*) Robinson, W. K., Carboni, C., Kloess, P., Perkins, S. P., and Coles, H. J., 1998, *Liq. Cryst.*, **25,** 301; (*i*) Guymon, C. A., Hoggan, E. N., Bowman, C. N., Clark, N. A., Rieker, T. P., and Walba, D. M., 1997, *Science*, **275,** 57.

[8] Merlo, A. A., Magnago, R. V., Vollmer, A. F., Mauler, R. S., Vargas, F., and Pesce, N. S., 1999, *Polym. Bull.*, **42,** 551.

[9] Merlo, A. A., Ritter, O. M. S., Pereira, F. V., Vieira, C. H., and da Silveira, N. P., 2001, *J. Braz. chem. Soc.*, **12,** 184.

[10] Merlo, A. A., Gallardo, H., and Taylor, T. R., 2001, *Química Nova*, **24,** 354.

[11] Wolfe, S., 1972, *Acct. chem. Res.*, **5,** 102.

[12] Simon, J. P., Arnaud, S., Bley, F., Bèrar, J. F., Caillot, B., Comparat, V., Geissler, E., de Geyer, A., Jeantey, P., Livet, F., and Okuda, H., 1997, *J. appl. Crystallogr.*, **30,** 900.

[13] (*a*) Koppenhoefer, B., and Schurig, V., 1987, *Org. Synth.*, **66,** 151; (*b*) Koppenhoefer, B., and Schurig, V., 1987, *Org. Synth.*, **66,** 160.

[14] Svensson, M., Helgee, B., Skarp, K., and Andersson, G., 1998, *J. mater. Chem.*, **8,** 353.

[15] Portugall, M., Ringsdorf, H., and Zentel, R., 1982, *Makromol. Chem.*, **183,** 2311.

[16] (*a*) Whitcombe, M. J., Davis, F. J., Gilbert, A., and Mitchell, G. R., 1991, *Polym. Commun.*, **32,** 380; (*b*) Yadav, K. V., and Fallis, A. G., 1986, *J. org. Chem.*, **51,** 3372.

[17] (*a*) Neises, B., and Steglich, W., 1978, *Angew. Chem. int. Ed. Engl.*, **17,** 522; (*b*) Neubert, M. E., Laskos, S. J., Maurer, L. J., Carlino, L. T., and Ferrato, J. P., 1978, *Mol. Cryst. liq. Cryst.*, **44,** 197.

[18] Carey, F. A., and Sundberg, R. J., 1993, *Advanced Organic Chemistry*, Part B (New York: Plenum Press), p. 244.

[19] Faustini, F., Demunari, S., Panzevi, A., Villa, V., and Gandolfi, C. A., 1981, *Tetrahedron Lett.*, **22,** 4533.

[20] Keck, R., and Rètey, J., 1980, *Helv. Chim. Acta*, **63,** 769.

[21] Serrano, J. L., Sierra, T., Ros, M. B., Ezcurra, A., and Zubia, J., 1992, *J. Am. chem. Soc.*, **114,** 7645.

[22] Mitsunobu, O., 1981, *Synthesis*, 1.

[23] Townsend, C. A., Salituro, G. M., Nguyen, L. T., and DiNovi, M. J., 1986, *Tetrahedron Lett.*, **27,** 3819.

[24] Flack, H. D., 1983, *Acta Cryst.*, **A39,** 876.

[25] Hsiue, G.-H., and Chen, J.-H., 1995, *Macromolecules*, **28,** 4366.

[26] Sheldrick, G. M., 1990, SHELXS-86: Program for the Solution of Crystal Structures, University of Göttingen, German.

[27] Sheldrick, G. M., 1997, SHELXL-97: Program for the Refinement of Crystal Structures, University of Göttingen, German.

[28] Zsolnai, L., 1995, ZORTEP: An Interactive Molecular Graphics Program, University of Heidelberg, Germany.

[29] Nardelli, M., 1995, *J. appl. Crystallogr.*, **28,** 659.

[30] Ebbutt, J., Richardson, R. M., Blackmore, J., and McDonnell, D. G., 1995, *Mol. Cryst. liq. Cryst.*, **261,** 549.

[31] Lam, J. W. Y., Kong, X., Dong, Y., Cheuk, K. K. L., Xu, K., and Tang, B. Z., 2000, *Macromolecules*, **33,** 5027.

[32] Noirez, L., Boeffel, C., and Daouad-Aladine, A., 1998, *Phys. Rev. Lett.*, **80,** 1453.

[33] Davidson, P., 1999, in *Liquid Crystals II*, edited by D. M. P. Mingos (Berlin: Springer Verlag), p. 1.

[34] Sutherland, H. H., and Rawas, A., 1986, *Mol. Cryst. liq. Cryst.*, **138,** 179.

[35] Dewar, M. J. S., Zoebisch, E. G., Horsley, E. F., and Stewart, J. J. P., 1985, *J. Am. chem. Soc.*, **107,** 3902.

[36] Couture, L., and Zitoun, R., 2000, *Statistical Thermodinamics and Properties of Matter* (Amsterdam: Gordon and Breach), p. 74.

[37] Davidson, P., 1996, *Prog. polym. Sci.*, **21,** 893.

[38] Bauman, D., Chrzumnicka, E., and Wolarz, E., 2000, *Mol. Cryst. liq. Cryst.*, **352,** 67.

[39] Borsali, R., Yoon, D. Y., and Pecora, R., 1998, *J. phys. Chem. B*, **102,** 6337.

[40] Berne, B. J., Pecora, R., 1976, *Dynamic Light Scattering* (New York: John Wiley), p. 191.